Correlation between experimental and analytic approaches to study the erosion rate of aluminum-metal matrix composites

M. Asaduzzaman Chowdhury*, U. Kumar Debnath*, M. Kchaou**'***, B. Ahmed Shuvho****, A. Rahman* and B. Kumar Roy*

* Dhaka University of Engineering and Technology, Gazipur, Bangladesh
** Department of Mechanical Engineering, College of Engineering, University of Bisha, Saudi Arabia
*** Laboratory of Electromechanical Systems (LASEM), National Engineering School of Sfax, University of Sfax, Tunisia
**** Department of Industrial & Production Engineering, National Institute of Textile engineering and Research (NITER), Savar, Dhaka, Bangladesh
,* Corresponding Author: kchaou.mohamed@yahoo.fr

ABSTRACT

The incorporation of a ceramic particles like SiC, Al2O3, and TiO2 into aluminum matrices results in aluminum composite with better mechanical and physical properties that make them attractive for various applications such as aircraft, helicopter, high-speed automobile, and submarine. In this study, the erosion properties of the aluminum composite were studied in dry conditions using sand blast-erosion test rig. Impact velocity, standoff distance, particle size, particulate (wt. %), and impingement angle were preferred as control factors. Taguchi method, Grey relational, and regression analysis were considered for optimizing the erosion process parameters. L27 orthogonal array was determined for the experimental trials. The most significant factors in the process were identified. Nonlinear regression model has been developed for Grey relational grade in relation to the different erosion parameters. An optimization schema is established based on a correlation between analytic and experimental results.

Keywords: Aluminum-metal matrix composites; Erosion rate; Optimization schema.

INTRODUCTION

Solid particle erosion, slurry erosion, friction, wear, and corrosion are the high concerning issues for surface engineering and tribology field. Erosion, wear friction, and lubrication of interfacing surfaces are the main topic of the interdisciplinary science of tribology, and wear rate evaluation is the most widely used technique for the failure analysis as well as to enhance service life (Thompson et al., 2009, Ozsarac et al., 2007). Attrition is one of the material removals processes from a solid surface because of mechanical interaction between the surfaces and impinged solid particles with dry compressed air or liquid. In the modern technological era, erosive damage of different materials is considered as a highly concern issue regarding the sustainability of the composite materials in the hostile conditions. In various engineering and industrial fields, the lightweight materials are used widely because of their low cost (Chowdhury et al., 2015). Due to the development of manufacturing techniques and the suitability or fitness to design

various systems and mechanisms, the aluminum composite is used widely in erosive wear environmental situations such as aircraft, helicopter, high-speed automobile, and submarine (Chowdhury et al., 2016, Shuvho et al., 2020a). Erosion rate is affected by various factors related to test conditions (impact velocity, impact angle, standoff distance, particle flux, temperature, nozzle geometry, and hardness of the materials, particles characteristics (erodent size, particles type, and size) and/or the material properties, particularly the hardness and the roughness (Shuvho et al., 2020a, Shuvho et al., 2020b, Noon et al., 2017). Most of the literature review suggested that impingement angle and impact velocity are two aspects that unusually effect the erosive behavior of different materials under different operating and processing parameters (Shuvho et al., 2019, Chowdhury et al., 2019, Chowdhury et al., 2017). However, it was not cleared, and in this connection, experimental results need to be analyzed under different proposed models and methods.

The aluminum composite is classified as a ductile material, as the higher erosion is obtained between impact angles 15–30 degree (Miller et al., 2006). It shows an erosive-corrosive wear behavior under wet conditions (Miller et al., 2006). Based on failure studies, an active relation between hardness and erosion mechanisms was noticed (Oka et al., 2005). Poor tribological properties were found in conventional aluminum alloys. However, reinforcing particles have a significant impact on reducing friction of coefficient as well as wear rate (Soy et al., 2011, Findik, 2014).

Design of Experiment (DOE) is the versatile used statistical tool applied in many areas such as engineering, agriculture, medical, fundamental science, design optimization, and prediction. Taguchi method is a well-established DOE tool utilized to study the effect of impact velocity, applied load, impingement angle, stand of distance, and reinforcement.

Selvi et al. (2015) investigated the wear rate of the Al based MMC through developing a mathematical model using second order response surface model, and the adequacy of their results was justified by using ANOVA.
Joshi et al. (2020) studied wear behavior of Al based MMC by utilizing the antlion algorithm (ALO) optimization technique, and the results were verified by using ANOVA, and the most influenced parameter was found to be load among the parameters such as reinforcement, sliding distance, sliding velocity, and applied load.

However, regarding the variability of factor conditioning erosion behavior, a prediction of the most potential parameters is required (Tzeng et al., 2009, Kuram et al., 2013). Therefore, an optimization schema should be developed to correlate relative relation and synergistic effect of such factors.

In this paper, the erosion behavior of aluminum composite is studied based on an experimental approach considering the variability of particles characteristics and operational parameters. The effect of applied load, impact velocity, impingement angle, stand of distance, and erodent size of the developed Al based MMC is analyzed using statistical tools. A new optimization schema based on a correlation between experimental results and Taguchi and Grey relational analysis methods is proposed to well study the erosion rate of the composite material.

MATERIALS AND METHODS

Materials Preparation and Erosion Measurement

The mechanical properties and chemical composition of the aluminium composite are listed in Tables 1 and 2. Aluminium composites reinforced with SiC, TiO_2, and Al_2O_3 were synthesized by stir casting moulding method since it is economical and simple techniques for manufacturing aluminium composites. The average size of the reinforcement particles is about 47 μm. The reinforcement particles SiC, TiO_2, and Al_2O_3 were collected from Merck KGaA, CMD Millipore Corporation, 290 Concord Road, Billerice MA01621, USA.

Square-shaped samples in the dimension of 50mm·30mm·5mm were processed by diamond cutter from injection molded plaques. The specimens are cleaned by acetone before erosion test. Sand abrasive particles with spherical shapes (300–355, 355–500, 500–600 microns of diameter) and hardness and density of these particles are 42, 43.2, and 44 MPa; 1436, 1440, and 1443 kg/m^3 respectively. The tested surface was thoroughly washed by using acetone solvent and a maximum level of precaution was maintained during core surface preparation before each test. A dryer has been utilized to control the moisture of the aluminium composites during the experiment, and 70% humidity was maintained. At the end of the experiment, the dust and sand particles affected the erodent surface of the specimen cleaned with dry air at a pressure of 6 bars. Dry quartz type silica (SiO_2) grain sizes 300–600 microns with irregular shapes including rounded, angular, and slightly rounded was utilized as an erodent particle. Motor type vibration sieve machine (model: VSS-T, Vinsyst Technologist, ISO 900, India) within the range 97μm to 4mm was utilized to determine the particle size. The weight of the specimens before and after erosion test was estimated using precise digital electronic balance (model: SP404D, Science tech Inc, USA).

Erosion rate was calculated through difference of before weight and after weight of the specimen with divided by time. Each experiment for each specimen was carried out for 10 minutes, and feed rate of erodent particles was maintained 5 gm/sec for all specimens.

Table 1. Chemical composition of Al6063-0, 7, 12% (SiC-Al2O3-TiO2).

Chemical Element	Wt. (%)	Chemical Element	Wt. (%)
Manganese (Mn)	0.0 - 0.10	Chromium (Cr)	0.0 - 0.10
Iron (Fe)	0.0 - 0.35	Copper (Cu)	0.0 - 0.10
Magnesium (Mg)	0.45 - 0.90	Other (Each)	0.0 - 0.05
Silicon (Si)	0.20 - 0.60	Others (Total)	0.0 - 0.15
Zinc (Zn)	0.0 - 0.10	Aluminum (Al)	Balance
Titanium (Ti)	0.0 - 0.10		

Table 2. Mechanical properties of the aluminum composite.

Property	Actual or measured data	Units
Density	2.729	gm/cc
Yield strength	113.4	N /mm^2
Average Impact Force	8.62	N-m
Ultimate Tensile Strength	148.618	N /mm^2
Hardness	98.56	HB

EROSION TEST

A sand blast erosion test rig was utilized to investigate the erosion properties of the composite materials as shown in Fig. 1. The ejection of abrasive particles is insured by a nozzle with controlled pressure a velocity. The double-disc technique was exploited to measure the impingement velocity of the solid particles as shown in Fig. 2. In fact, sand particles moved along hollow space of the rigid upper disk, which in turn causes damage (A) in the lower rigd disc (B). When two discs rotate, then then second damage (B) occurred on the lower disc. The angular displacements of A and B were calculated using Equation (1).

$$V = \frac{2\pi RvL}{S}$$
(1)

where L is the distance between two discs, V is the speed of the two plates, S is noted as the angular distance between two colors damage, and R is the radius from the center of the lower plate to point B. The impact speed is calibrated at different conditions are mentioned in Shuvho et al. (2006).
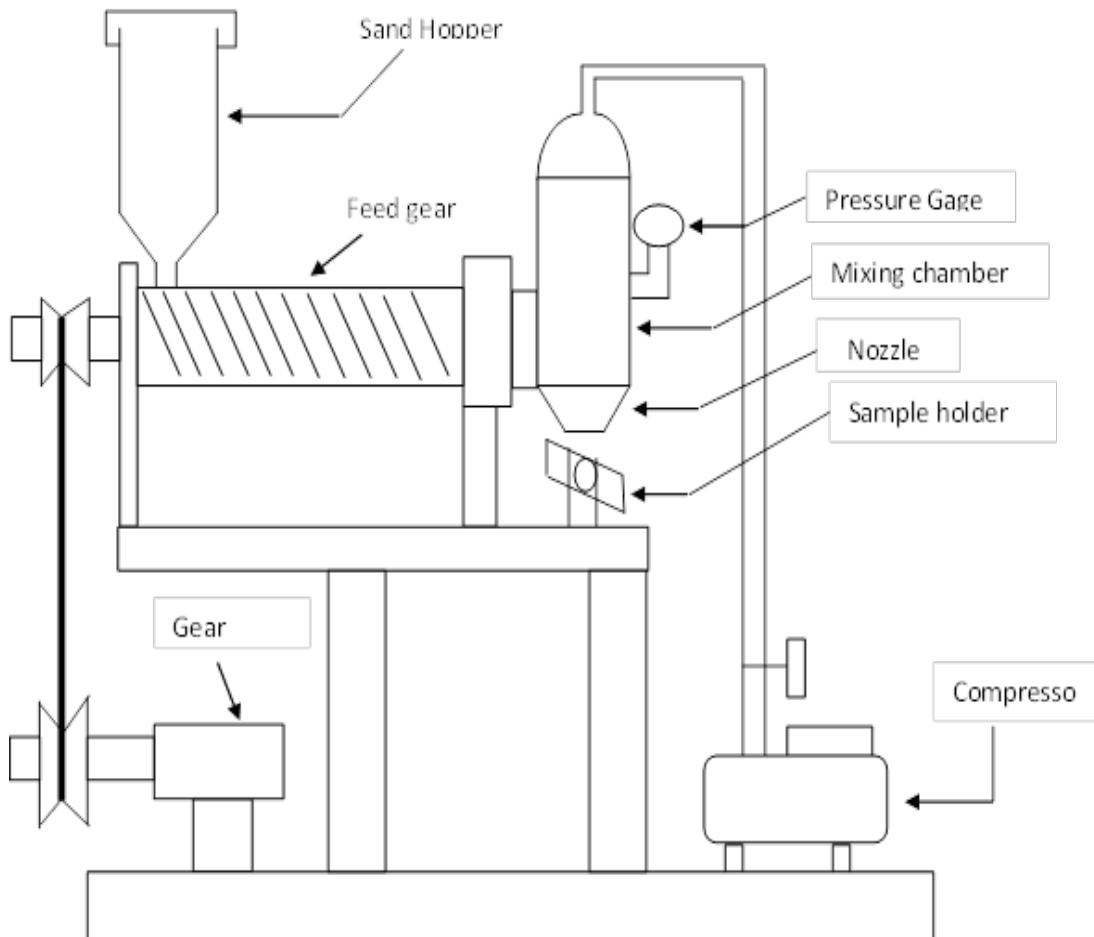

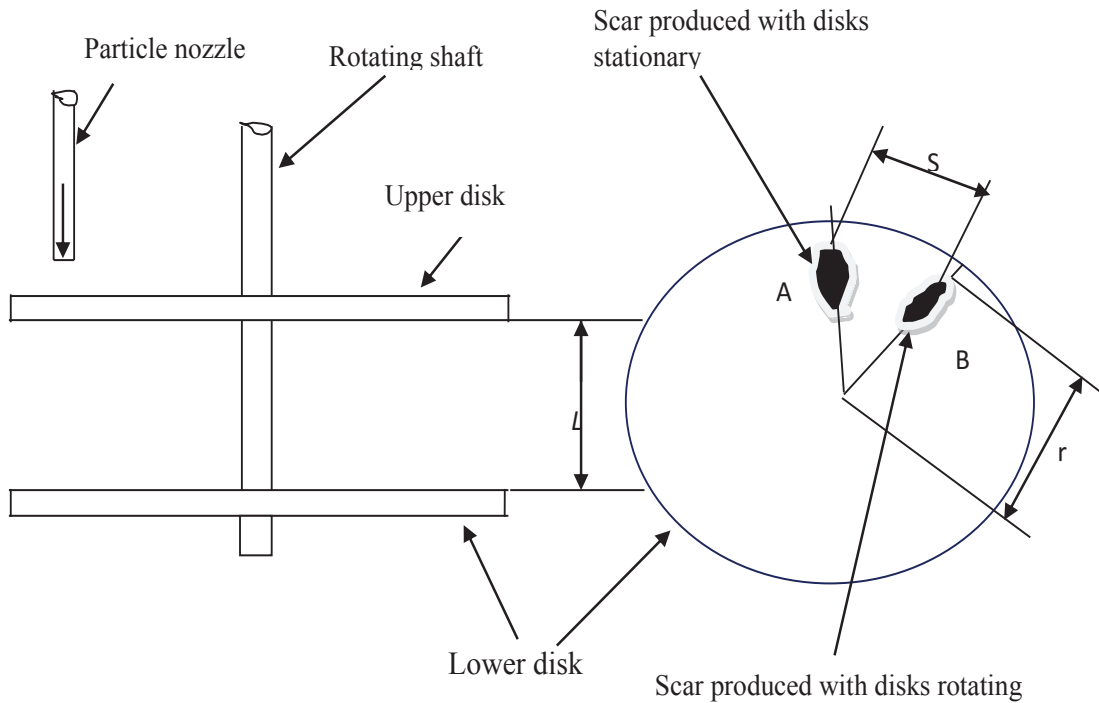**Figure 1.** Depiction of the solid particle erosion test rig.

Figure 2. Depiction of the experimentation used for measuring impact velocity.

CHOICE OF THE EXPERIMENTAL PARAMETERS

Taguchi method is used to fix and control experimental parameters. Considering the Taguchi's L27 orthogonal array (OA) design concept (Kuram et al., 2014), the five influential variable factors such as impact velocity, impingement angle, stand of distance, erodent size, and particulates (wt. %) at three different levels as shown in Table 3 are designated. The number of experiments is defined by S/N ratio (signal-to-noise) (Bagci et al., 2015), depending on the trends of experimental data. As the minimum amount of erosion rate is desired for practical implications, the condition for S/N ratio is taken, as the smaller the better. Considering this logic, a logarithmic formulation of the loss function is determined as follows. In the case where the smaller the erosion rate, the better, the quality level of materials can be calculated using Equation (2).

$$\frac{S}{N} = -10 log \frac{1}{n} \left(\sum y^2 \right) \tag{2}$$

where *n* is the amount of experimental data, and y is the observed data. Less amount of erosion ensures better characteristics, which can be correlated with S/N ratio transformation concept (Patnaik et al., 2010, Mahapatra et al., 2009). There are two experimental factors such as signal and noise: one is fixed in nature, and the other one is varied to investigate the erosion rate. The different level of controlled parameters is considered for designing the system for the Taguchi method. Those combinations are mentioned in Table 3. Experimental results of erosion rate are converted into S/N ratio following L27 Orthogonal array shown in Table 4.

Table 3. Fixed and controlled parameters for experimentation.

Fixed parameters Fixed conditions/values		Control factor	Symbol	Level		
				I	II	III
Nozzle diameter(mm)	5	Velocity of impact (m/sec)	A	30	40	50
Length of nozzle(mm)	55	Angle of impingement (Degree)	B	30	60	90
Erodent	Silica sand under dry condition	Erodent size (Micron)	C	300-355	355-500	500-600
Erodent shape	Irregular	Standoff distance (mm)	D	15	20	25
Test temperature	Room temperature	Composite Particulate-wt(%)	E	0	7	12
Erodent feed rate gm/sec	4.56					
Erodent micro-hardness (HV)	42-44					

Table 4. Conversion of experimental results into S/N ratio.

Si no	Impact Velocity (m/s)	Impingement Angle (degree)	Erosion particle size(mm)	Stand -off Distance (mm)	Composite Particulate-wt(%)	Erosion Rate (mg/kg)	S/N Ratio
1	30	30	300-355	15	0	180.87	-45.15
2	30	30	300-355	15	7	75.11	-37.51
3	30	30	300-355	15	12	33.20	-30.42
4	30	60	355-500	20	0	127.88	-42.14
5	30	60	355-500	20	7	38.41	-31.69

6	30	60	355-500	20	12	19.21	-25.67
7	30	90	500-600	25	0	159.47	-44.05
8	30	90	500-600	25	7	60.97	-35.70
9	30	90	500-600	25	12	33.77	-30.57
10	40	30	355-500	25	0	124.95	-41.93
11	40	30	355-500	25	7	43.35	-32.74
12	40	30	355-500	25	12	23.92	-27.58
13	40	60	500-600	15	0	204.83	-46.23
14	40	60	500-600	15	7	90.56	-39.14
15	40	60	500-600	15	12	43.18	-32.71
16	40	90	300-355	20	0	191.48	-45.64
17	40	90	300-355	20	7	67.66	-36.61
18	40	90	300-355	20	12	67.66	-36.61
19	50	30	500-600	20	0	255.04	-48.13
20	50	30	500-600	20	7	90.45	-39.13
21	50	30	500-600	20	12	45.47	-33.16
22	50	60	300-355	25	0	210.26	-46.46
23	50	60	300-355	25	7	57.95	-35.26
24	50	60	300-355	25	12	37.31	-31.44
25	50	90	355-500	15	0	229.48	-47.21
26	50	90	355-500	15	7	75.58	-37.57
27	50	90	355-500	15	12	42.38	-32.54

Selection of the Needed Number of Observations

The number of observations (i.e., number of experiments) for grey Taguchi method is calculated to determine the actual number of observations for maintaining certain level of confidence with desired percentage accuracy level using Equation (3).

$$n = [\frac{zs}{A\bar{x}}]^2 \tag{3}$$

where n is the number of experiments for confirming the requisite accuracy. Normally distributed deviate is symbolized by Z for required level of confidence. The projected standard deviation S is given by Equation 4. A implies precise accuracy that is indicated as a decimal fraction of trusted value of $\bar{x}$ (mean value of erosion

measured), and $n^/$ is the number of experimentations at similar conditions that has been previously done. The required number of experimentations is determined by Equation 3. In this case, 95% level of confidence in the range of 2% accuracy was assumed.

$$\sqrt{((\sum x^2 - (\sum x)^2 / n^/)/(n^/ - 1))} \tag{4}$$

RESULTS AND DISCUSSION

Grey Taguchı Method

The steps of Grey Taguchi Method are summerized in Fig. 3. Firstly, experimental values, i.e., velocity of the impact z (m/s), angle of impingement (degree), erodent size (micron), standoff distance (mm), and composite particulate-wt (%), are considered to determine the number of contributions to maximize erosion rate of the tested aluminum composite. Secondly, grey correlation coefficients are measured after grey data preprocessing. A series of different units is replaced as dimensionless parameters. In general, each series is normalized by dividing the value of the real series by their mean. The analogy of the arrangements of the real reference value the theoretical data is presented as $X_0(k)$ and $X_i(k)$, i=1, 2, . . ., m; k=1, 2, . . ., n, respectively, where *m* is the number of the tests to be done, and *n* is the total amount of observation data. Data are preprocessing and reorganize the real arreangement to a comparable arrengement.   Since the Grey Taguchi method represents the level of correlation between the comparability sequences and references, the higher Grey relational grades show that the comparability squence demonstrates strong correlation with the reference sequence.
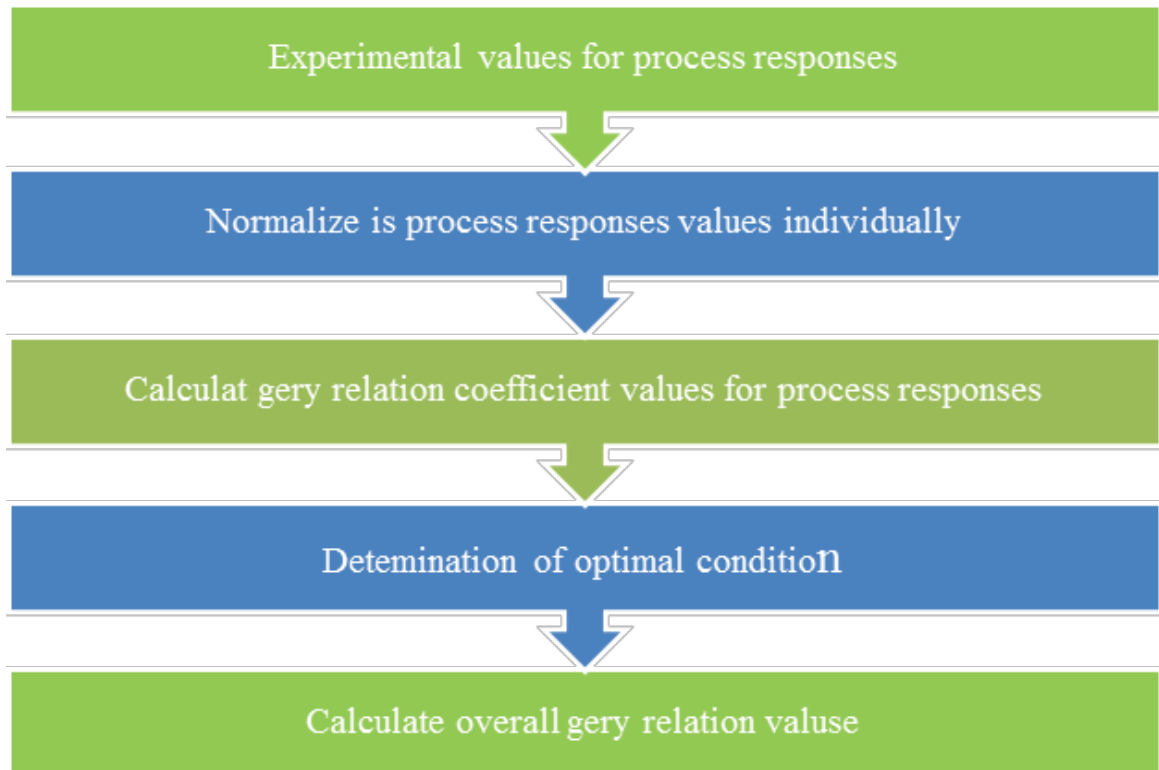

Figure 3. Steps of grey taguchi analysis method.

Normalızatıon of Experımental Results

Based on Table 4, normalization data for the erosion rate response need to be considered. Through normalization, data is preprocessed, which is called gray relational generating. Data normalization process is also carried out based on the quality characteristics of the response. The smaller the quality characteristic of the erosion rate, the better. Each value of the experimental results is normalized in the range of 0 to 1 using Equation 5.

$$X_i(M) = \frac{MaxY_i(M) - Y_i(M)}{MaxY_i(M) - MinY_i(M)} \tag{5}$$

where

$X_i(M)$ =Value after normalizing data.
Max $Y_i(M)$ = Largest value of $Y_i(M)$ for M^{th} response.
Min $Y_i(M)$ = Smallest value of $Y_i(M)$ for M^{th} response.

Grey Relatıon Coeffıcıents

The calculation of the gray relational coefficient value of erosion rate is presented in Table 5. Equation (5) is used to calculate the Grey relation coefficient. The rank is arranged by observing the value of Grey relational coefficient for understanding the range of minimum to maximum erosion rate using grey grade concept. These results are listed in Table 6.

$$\sum_i(M) = \frac{\Delta_{min} + \psi\Delta_{max}}{\Delta_{oi}(M) + \psi\Delta_{max}} \tag{5}$$

where Δ_{oi} =Quality loss function
$\Delta_{oi} = [Xoi(M) - Xi(M)]$
Δ_{min} =the minimum values of the differences of Δ_{oi}
Δ_{max} =the maximum values of the differences of Δ_{oi}
ψ = Value between 0 to 1, its value is usually considered 0.5 in literature (Patnaik et al., 2010, Mahapatra et al., 2009).

Table 5. The impact velocity calibration at various pressures.

Pressure (bar)	Speed of the rotating disc (rpm)	Linear separation of two marks (mm)	Impact velocity (m/s)	Average impact velocity (m/s)
3.5	4700	6.2	49.61	50
		6.3	48.83	
		6.1	50.42	
3	4500	7.4	39.98	40
		7.2	40.88	
		7.4	39.78	
2	4000	8.7	30.07	30
		8.5	30.75	
		8.6	30.42	

Table 6. Rank selection from Grey relational coefficient using grey grade concept.

Run No	Erosion rate (mg/kg)	Normalized values for erosion rate	$\Delta_{oi}(M)$	Grey relational coefficient	Rank
1	180.87	0.314506	0.685494	0.421765	22
2	75.11	0.762965	0.237035	0.678394	15
3	33.20	0.940678	0.059322	0.893939	3
4	127.88	0.539202	0.460798	0.520401	20
5	38.41	0.918585	0.081415	0.859972	6
6	19.21	1	0	1	1
7	159.47	0.40525	0.59475	0.456725	21
8	60.97	0.822923	0.177077	0.738469	12
9	33.77	0.938261	0.061739	0.890092	4
10	124.95	0.551626	0.448374	0.527218	19
11	43.35	0.897638	0.102362	0.830066	9
12	23.92	0.980028	0.019972	0.96159	2
13	204.83	0.212908	0.787092	0.388472	24
14	90.56	0.697452	0.302548	0.623015	18
15	43.18	0.898359	0.101641	0.83106	8
16	191.48	0.269516	0.730484	0.406344	23
17	67.66	0.794555	0.205445	0.708773	13
18	67.66	0.794555	0.205445	0.708773	14
19	255.04	0	1	0.333333	27
20	90.45	0.697918	0.302082	0.623378	17
21	45.47	0.888649	0.111351	0.81786	10
22	210.26	0.189883	0.810117	0.381645	25
23	57.95	0.835729	0.164271	0.752705	11
24	37.31	0.92325	0.07675	0.866926	5
25	229.48	0.108383	0.891617	0.359294	26
26	75.58	0.760972	0.239028	0.676564	16
27	42.38	0.901751	0.098249	0.835773	7

Response Table for Erosıon Rate

In response data, Table 7 ranks square measure distributed for technique parameters supporting the delta values. The delta value is the distinction between the lowest and highest average values of every method parameter. The rank designates the significance of every issues of the response. The ranks and delta values show that Pulse on time has the highest result on erosion rate and is followed by standoff distance, impact velocity, particle size, impingement angle, and composite particulate wt %. From the grey relational grade table, the optimum parametric combination was found. The optimal setting factors are A1, B2, C2, D3, and E3.

Table 7. Responses for grey relational grade (means).

Level	Impact velocity	Impingement angle	Particle size	Standoff distance	Composite Particulate-wt(%)
1	0.717751	0.676394	0.646585	0.634253	0.421688
2	0.665035	0.691577	0.730098	0.664315	0.721259
3	0.627498	0.642312	0.633001	0.711715	0.867334
Δ	0.090253	0.049265	0.097097	0.077462	0.445646
Rank	3	5	2	4	1

Anova for Grey Relational Grade

Analysis of variance is a decesive statistical technique, which can be practiced finding out the individual interactions of related control factors taken fromm experimental results. ANOVA determines the dominating factors on erosion as a contributor. The summarized results derived from this analysis are illustrated in Table 8 and Table 9. In ANOVA technique, a 95% assurance level and 5% of significance level were considered. P-values obtained for the control factors demonstrate the significance of these factors on erosion rate. The P-values for each factor mean that the impacts of impingement angle, impingement velocity, erodent size, standoff distance, and composite particulate are significant. These results are in agreement with the results of Mahapatra et al. (2009), which disclose that the impact velocity and composite particulate have noticeable effects on the erosion rate even though the effect of impingement angle is not very prominent. The graphical representation of S/N ratio is illustrated in Fig. 4, which indicates the consequence of the four variables on erosion. A simple model is needed to be designed for predicting the performance of the probable interrelationships among the parameters. In this case, MINITAB 17 is used. Comparing the interactions mentioned in Fig. 5, it can be suggested that the interaction of A× E is the most dominating combination on erosion but not very crucial for the combined effects of E×C and E×D. The regression model fitted for the erosion rate is represented by Equation 6. The results of Table 6 obtained from Grey analysis indicate that the maximum influencing parameter is composite particulate wt(%), which can vary erosion rate significantly. This observation is also proven in experimental results; that is, as the Composite Particulate wt (%) decreases, erosion rate increases. Similar findings are obtained under ANOVA analysis shown in Table 7 and illustrated in Figs. 2 and 4. In this contest, it can be stated that two different methods are in compliance with the experimental results.

Erosion rate=125.1 + 1.750 Impact velocity (m/sec) + 0.104 Impingement angle (Degree) + 0.0679 Particle size (μm) - 2.48 Standoff distance(mm) - 12.70 Composite Particulate wt. (%) (6).
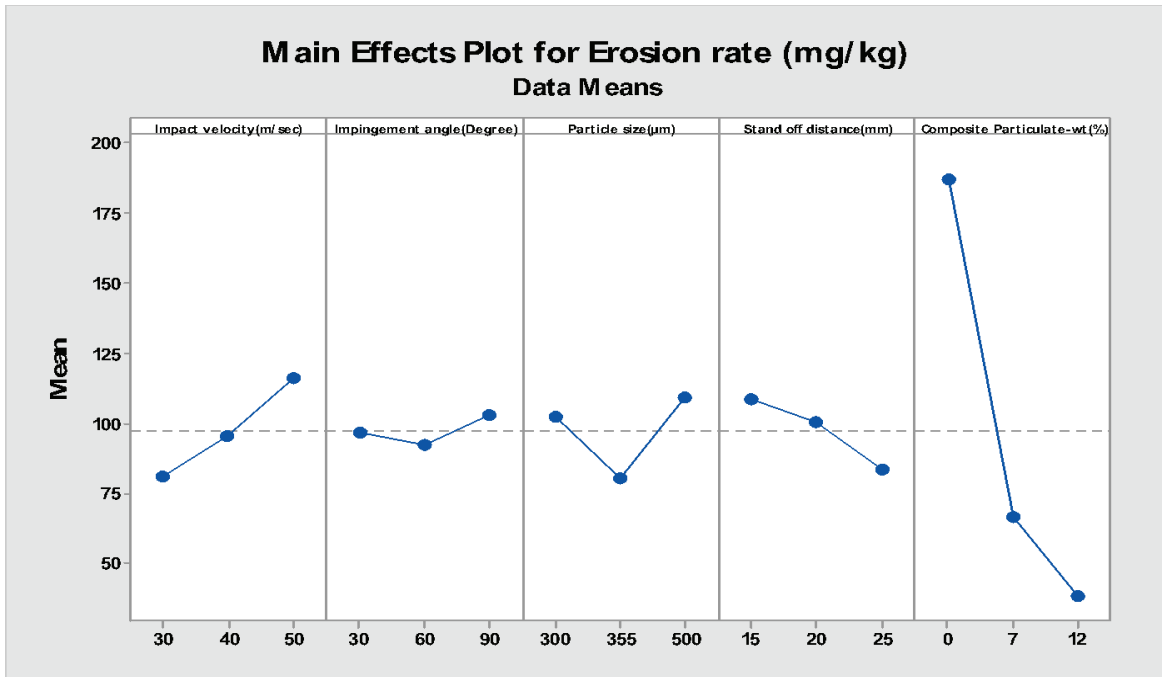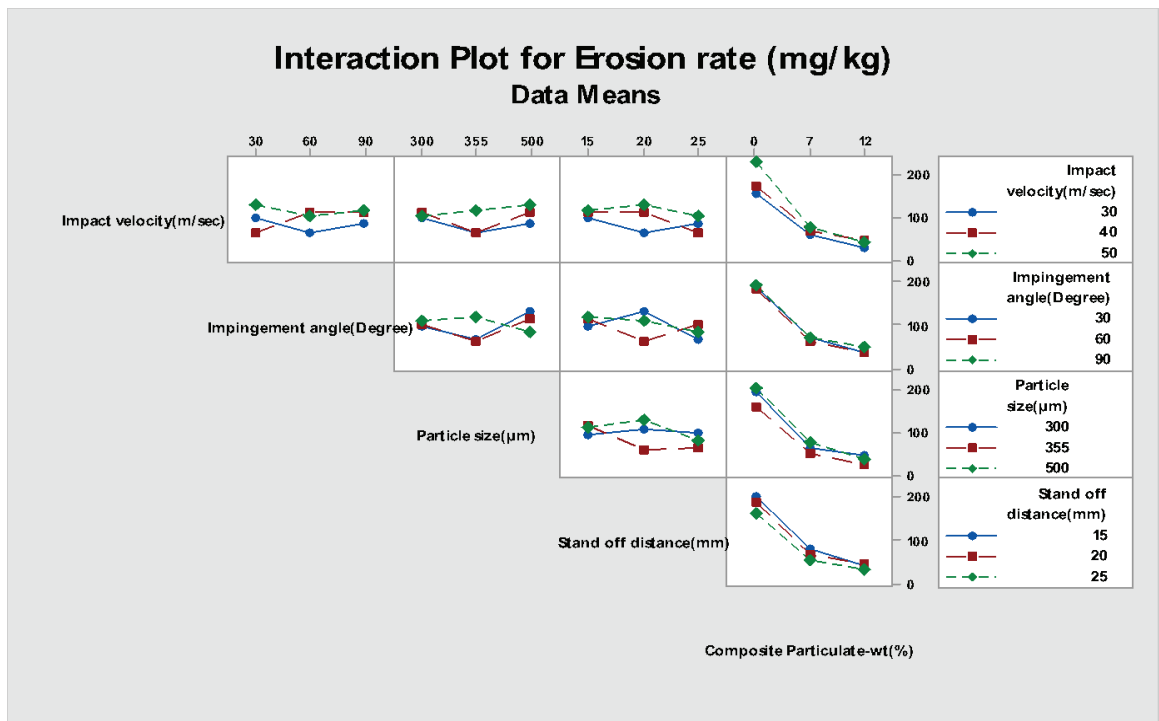
Figure 4. Mean effects plot for erosion rate.

Figure 5. Interaction plot for erosion rate.

Table 8. Analysis of the Variance.

Source	DF	Adj SS	Adj MS	F-value	P-Value	% Contribution
Impact velocity(m/sec)	2	5575	2787.5	60.90	0.008	4.223069
Impingement angle(Degree)	2	546	273.1	5.97	0.535	0.413596
Particle size(μm)	2	4048	2023.8	44.22	0.023	3.066365
Standoff distance(mm)	2	2885	1442.7	31.52	0.057	2.185391
Composite Particulate-wt(%)	2	112248	56123.9	1226.16	0.000	85.02799
Impact velocity (m/sec)*Composite Particulate-wt(%)	4	4637	1159.2	25.33	0.004	3.51253
Particle size (μm)*Composite Particulate-wt(%)	4	988	246.9	5.39	0.066	0.748411
Standoff distance (mm)*Composite Particulate-wt(%)	4	903	225.7	4.93	0.076	0.684023
Error	16	183	45.8			0.138622
Total	26	132013				100

Table 9. Model summary.

S	R-Sq	R-sq (adj)	R-sq (pred)
6.76551	99.86%	99.10%	93.68%

Conformation Test

The confirmation tests are considered for identifying the optimal parameters of control variables in the levels of I, II, and III. This test is significant in determining the quality characteristics of the erosion rate at different operating conditions. Experiment no. 6 (Table 6) mentions the highest grey relational grade, which is useful for selecting the optimal process parameter set of A1, B2, C2, D3, and E3. These can be identified as the best multiple performance aspects among the twenty-seven experiments for validating the experimental results with the theoretical one. Table 10 presents the comparison of the experimental values utilizing the orthogonal array of A1, B2, C2, D2, and E3 and theoretical results of grey optimal parameters of A1, B2, C2, D3, and E3 for erosion rate. The results of this study are compared with the study of other researchers as shown in Table 11, although the wear modes were different in different studies (Chowdhury et al., 2019, Chowdhury et al., 2016, Mahapatra et al., 2009) summarized in Table 11.

**Table 10.** Optimal process parameters.

	Optimal process parameters	
	Orthogonal array	**Grey theory design**
Level	A1, B2, C2, D2, E3	A1, B2, C2, D3, E3
Erosion	19.21	18.95

**Table 11.** Comparison of the results with the other studies.

Process	Experimental and design conditions	Optimal parameters	Grey theory design
Erosion (Chowdhury et al., 2015)	Impact velocity(A), Particle size (C), Standoff distance(D) and Composite Particulate-wt(%)(E)	A1,B2,C2,D2, E3	18.95 mg/kg
Turning process parameters (Tzeng et al., 2009)	Cutting speed(A), Feed Rate(B), depth of cut(C) and Cutting fluid mixture ratios(D)	A2, B1, C3, D3	1.0280 µm
Micro-mechanical machining processes (Kuram et al., 2013)	Spindle speed (A), Feed per tooth(B) and Depth of cut (C)	A1, B1, C1	0.33µm
Erosion (Chowdhury et al., 2016)	Impact velocity(A), Impact angle(B), Particle size (C) and Standoff distance(D)	A1,B2,C2,D2	1300.07 mg/gm
Wire cut (Ramanan et al., 2017)	Discharge current (IA), pulse on time (Ton), Pulse off time (Toff) and Servo speed rate (rpm)	A1,B3,C3,D1	0.7972 gm/min
Turning (Senthilkumar et al., 2015)	Cutting speed, Feed rate, Depth of cut, Approach angle	V2,f1,d1,A1	0.941 gm/min

Combined Effects of Operating Parameters on Erosion

Figure 6 indicates the surface plots and counter plots for the erosion at different conditions. Fig. 6(a) and 6(b) illustrate the surface plot and counter plot of erosion at impact velocity and impingement angle. The 3D photographs imply that responses are minimum for erosion rate at low level of impact velocity and impingement angle, whereas maximum erosion occurs at higher velocity and impingement Angele. Fig. 6(c) and 6(d) demonstrate the surface plots and counter plot of erosion at impact velocity and particle size. Maximum erosion rate is traced at high impact velocity and particle size. Fig. 6(e) and Fig. 6(f) reveal the surface plot and counter plot of erosion in combination of the impact velocity and standoff distance. A minimum material is pulled out at minimum impact velocity and stand of distance. Fig. 6(g) and Fig. 6(h) show surface plot and counter plot for erosion at impact velocity and composite particulate wt. %. Maximum erosion rate has been observed at lower composite particulate wt. %.
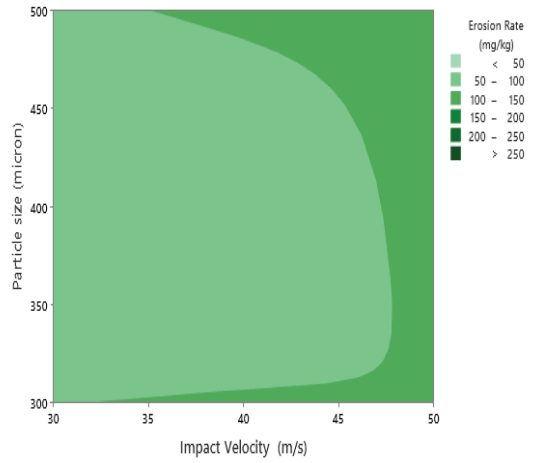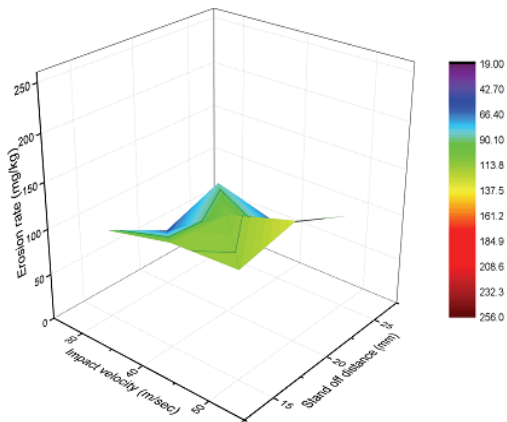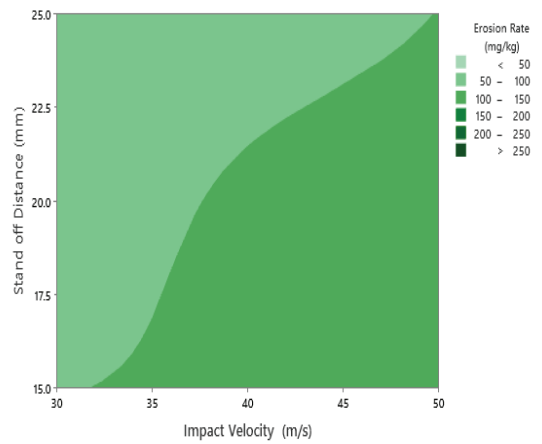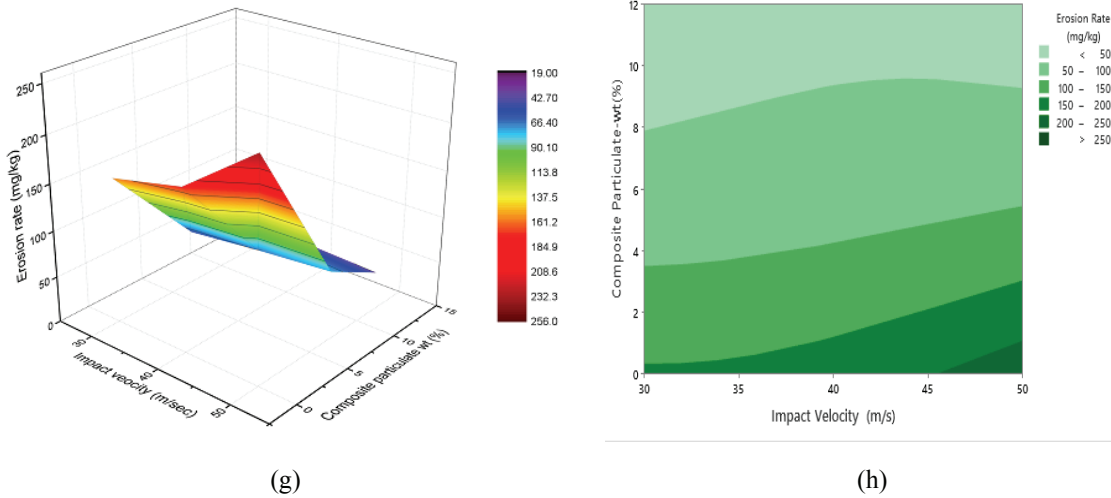
(a)

(b)

©

(d)

(e)

(f)

(g)

(h)
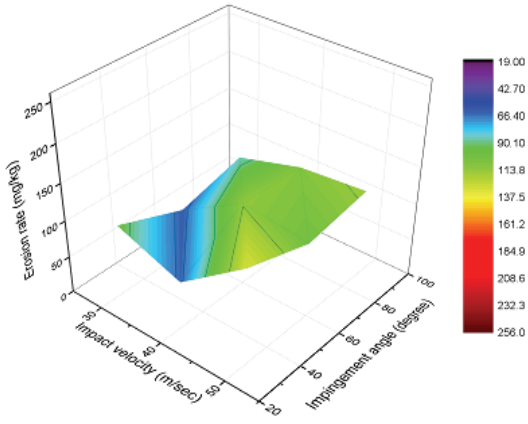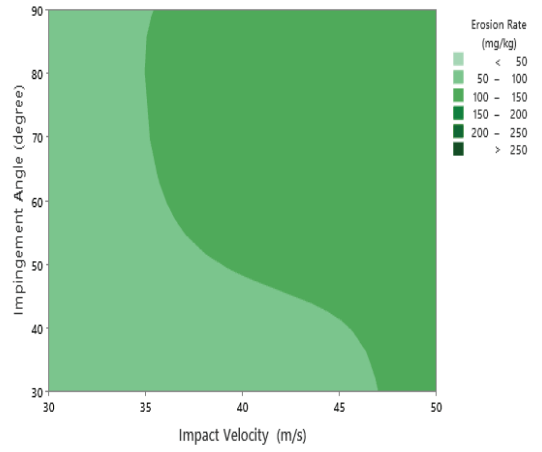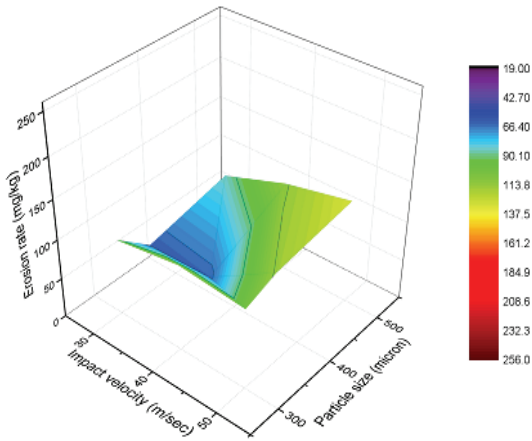
Figure 6. Surface plot of erosion (a, c, e, and g), and contour plot of erosion rate (b, d, f, and h).

Morphology Analysis

The morphology of eroded surfaces of aluminum-based composite was characterized by JEOL JSM 7600F Scanning Electron Microscope. SEM micrographs of aluminum composite are illustrated in Fig. 1 (a, b, c). The grooves, microploughing, displaced material, crater formation, and microcracks are visualized. These may appear due to the effect of kinetic energy, which is produced during striking of solid particles at high impact pressure on the test samples as seen in Fig. 7(a). Figure 7(b) implies the damaged surface due to absorbing the energy waves, which occurred by the action of impinging particles. Plastic deformation is observed at 60° impingement angle, and microcutting action and craters are also generated as seen in Fig. 7(b).
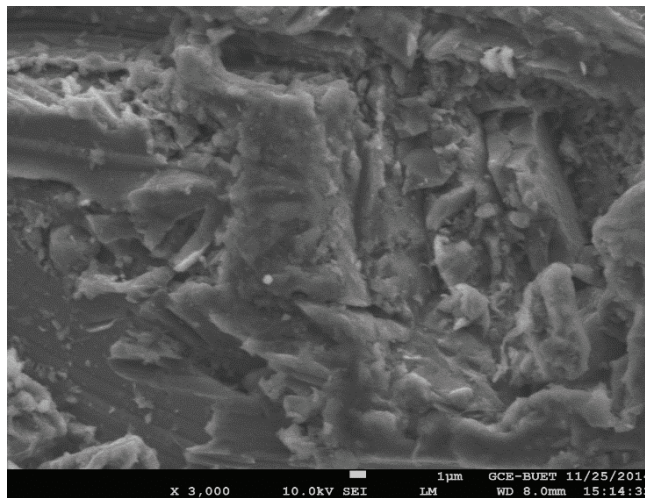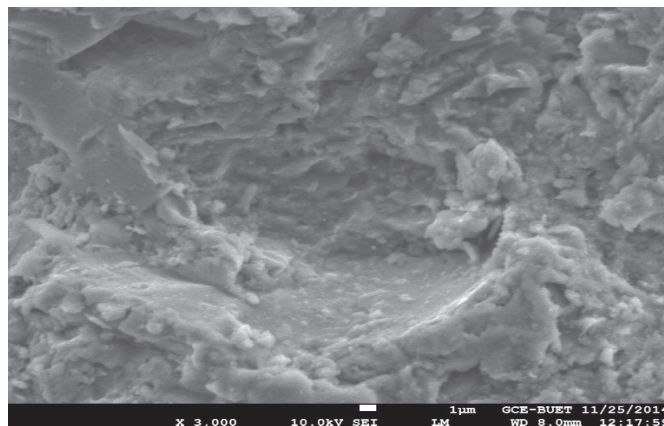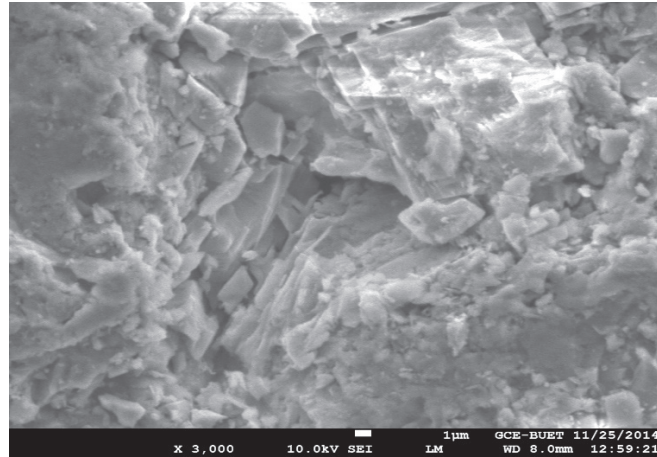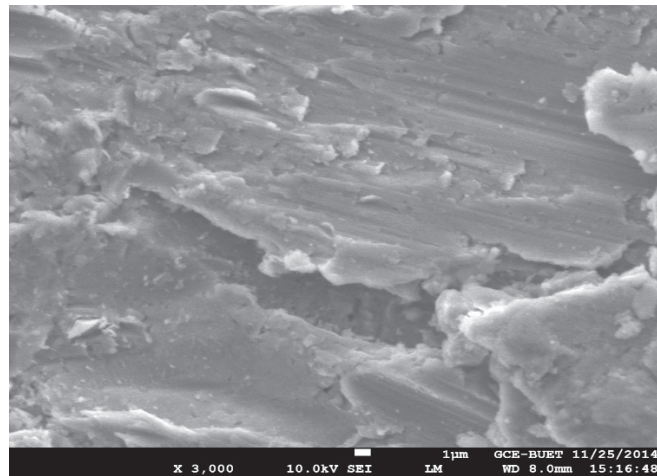

(a)
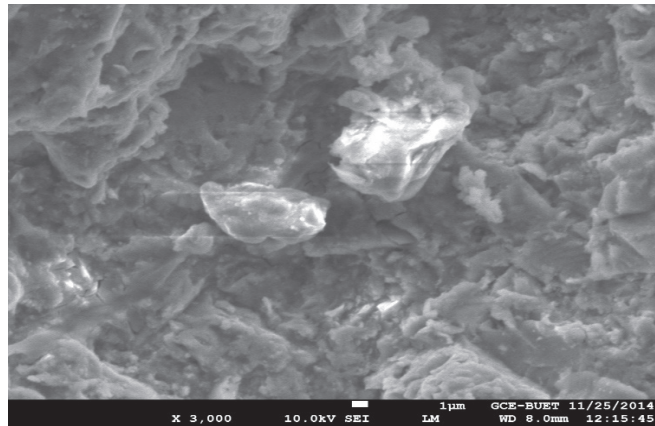
(b)
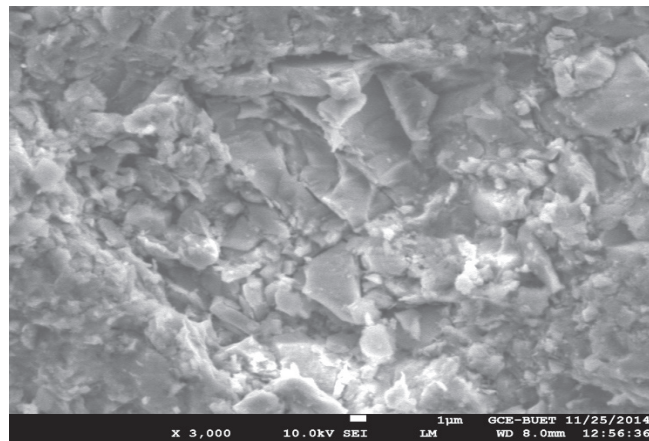
(c)

Figure 7. SEM observations of eroded aluminum composites at different impact angles: (a) 15 degree, (b) 30 degree, (c) 60 degree. [particle size 500-600 micron, impact velocity 30 m/s, stand of distance 15 mm].

(a)

(b)

(c)

Figure 8. SEM observations of eroded aluminum composite at various impact velocities: (a) 30 m/sec, (b) 40 m/sec, (c) 50 m/sec[partical size 500-600 micron, impact angle 30 degree, stand of distance 15 mm].

In Fig. 7(c), maximum erosion and surface damage happened at 90-degree impingement angle. Surface topography is shown in Fig. 8 (a, b, c) at distinctive velocities for following the wear mechanism. At 30 m/sec, a small amount of erosion rate is seen due to pullout and displaced material as seen in Fig. 8 (a). Pitting action is also responsible for lower erosion rate due to the low particle energy. Figure 8(b) indicates that the damage has been propagated on the target surface (at 40 m/sec). The damage is due to craters and pitting action. At 50 m/sec, crack and ploughing effects were detected. At high velocity, large amounts of ejected particles are seen for the impact of high particle energy shown in Fig. 8(c).

Energy Dispersive X-ray (EDS) Analysis

For elemental quantifying and mapping, energy dispersive X-ray spectroscopy (EDS) is a standard tool for a specified material. In this study, EDS mapping analysis was conducted out to investigate the elements contained in the composites and the proportions as shown in Fig. 9. The EDS mapping figure shows proportions of the composite's elements such as Al, C, O, Si, and Ti at different percentages, which confirmed the existence of Al_2O_3, SiC, and TiO_2 as reinforcement particles.
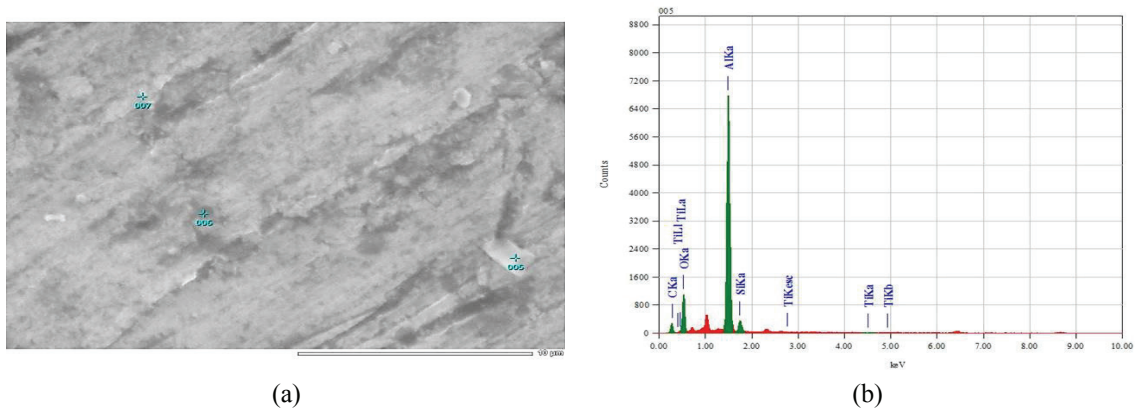

(a)   (b)

Figure 9. Elemental analysis using EDS mapping of aluminum based MMC.

FTIR Analysis of the Composite

For ascertaining the chemical functional groups in a specimen, Fourier transform infrared spectroscopy (FTIR) is a vast technique as a nondestructive testing tool. In FTIR spectra shown in Fig. 10 of the aluminum based MMC, the observed peak at 1570 cm-1 coincides with typical pyrrole ring vibration as discussed in Radhakrishnan et al. (2009). At low intensity peaks, 780 cm-1 is ascribed to =CH plane and out of plane vibrations and at 1480 cm-1 due to =CH plane vibrations (Saravanan et al., 2007). The stretching bond vibration OH shown in 3345 cm-1 for SiC and TiO2 and the absorption of CH functional group is seen at 2780 cm-1. C=C bond is seen at 1720 cm-1 due to the shifting vibration.
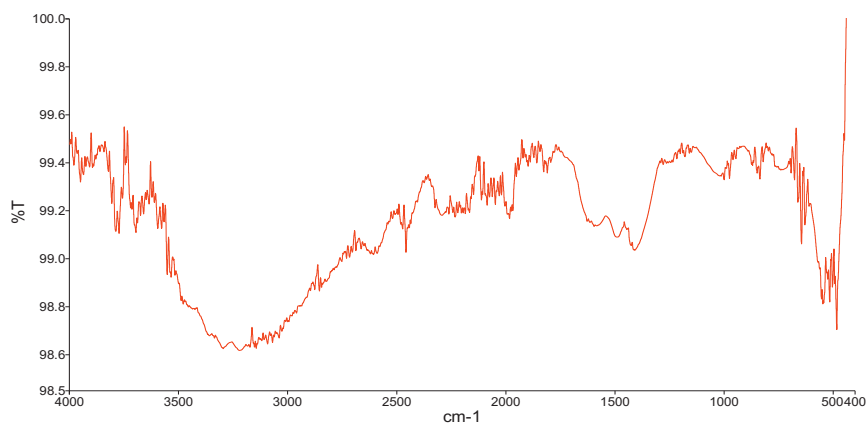

Figure 10. FTIR spectra of the Aluminum based MMC.

CONCLUSION

Composite particulates wt(%) are considereed as exceedingly influential and deciding grey grate factor for minimizing the erosion rate. The minimum erosion of 19.21 and 18.25 is obtained using an orthogonal array and grey rational analysis under optimized operating parameters (A1, B2, C2, D2, and E3). The novelty of the paper is that there are a lot of factors that affect the erosive behavior of different systems and mechanisms; however, the selection of most influential controlling parameters is important for erosive mechanisms. In automotive, aerospace, and windmill fields, the construction materials are extremely important to choose. As the main concerning issue is life cycles or life period of any materials for such types of industries, it will be extremely cost effective if the significant propogating factors are determined. If the factor is determined by modeling with the grey rational analysis, then it will be easy for the researchers to minimize or maximize the effect of parameters incorporating alternative materials or systems. In ANOVA analysis, almost 85% contributions on erosion rate are found in the case of composite particulate wt. (%) rather than other factors. As the influences of different operating parameters can be predicted using this method, in future, the outcome of the results can be utilized for designing mechanical and tribological processes, where erosive wear is concerning issues. Morphology, EDS, and FTIR studies produced consistent results regarding the aluminum-based composites materials. Various elements were confirmed by utilizing EDS mapping. Different chemical vibrational, nonvibrational, and stretching peak values were identified by the exploration of the FTIR analysis.

REFERENCES

Bagci, M. and H. Imrek, Application of Taguchi method on optimization of testing parameters for the erosion of glass fiber reinforced epoxy composite materials. Materials & Design, 2013. 46: p. 706-712.

Biswas, S. and A. Satapathy, 2010, A study on tribological behavior of alumina-filled glass–epoxy composites using Taguchi experimental design. Tribology Transactions, 53(4): p. 520-532.

Chowdhury, M.A., et al., 2015, Experimental evaluation of erosion of gunmetal under asymmetrically shaped sand particle. Advances in Tribology, 31 pages, ID 815179.

Chowdhury, M.A., et al., 2016, Experimental analysis of aluminum alloy under solid particle erosion process. Proceedings of the Institution of Mechanical Engineers, Part J: Journal of Engineering Tribology, 230(12): p. 1516-1541.

Chowdhury, M. A., Shuvho, B. A., Debnath, U. K., & Nuruzzaman, D. M. (2019). Prediction and Optimization of Erosion Rate of Carbon Fiber–Reinforced Ebonite Using Fuzzy Logic. Journal of Testing and Evaluation, 47(2), 1244-1258.

Chowdhury, M.A., et al., 2017, Erosion of mild steel for engineering design and applications. Journal of Bio-and Tribo-Corrosion, 3(3): p. 34.

Findik, F., 2014. Latest progress on tribological properties of industrial materials. *Materials & Design*, 57, pp.218-244.

Joshi, A.G., Manjaiah, M., Basavarajappa, S. and Suresh, R., 2020. Wear Performance Optimization of SiC-Gr Reinforced Al Hybrid Metal Matrix Composites Using Integrated Regression-Antlion Algorithm. *Silicon*, pp.1-11.

Kuram, E. and B. Ozcelik, 2013, Multi-objective optimization using Taguchi based grey relational analysis for micro-milling of Al 7075 material with ball nose end mill. Measurement. 46(6): p. 1849-1864.

Mahapatra, S. and A. Patnaik, 2009, Study on mechanical and erosion wear behavior of hybrid composites using Taguchi experimental design. Materials & Design. 30(8): p. 2791-2801.

Miller, A.E. and D. Maijer, 2006, Investigation of erosive-corrosive wear in the low pressure die casting of aluminum A356. Materials Science and Engineering: A, 435: p. 100-111.

Noon, A.A. and M.-H. Kim, 2017, Erosion wear on Francis turbine components due to sediment flow. Wear. 378: p. 126-135.

Oka, Y. and T. Yoshida, 2005, Practical estimation of erosion damage caused by solid particle impact: Part 2: Mechanical properties of materials directly associated with erosion damage. Wear, 259(1-6): p. 102-109.

Ozsarac, U., Findik, F. and Durman, M., 2007. The wear behaviour investigation of sliding bearings with a designed testing machine. *Materials & design*, *28*(1), pp.345-350.

Patnaik, A., et al., 2010, Solid particle erosion wears characteristics of fiber and particulate filled polymer composites: A review. Wear. 268(1-2): p. 249-263.

Radhakrishnan, S., Sonawane, N., & Siju, C. R. (2009). Epoxy powder coatings containing polyaniline for enhanced corrosion protection. Progress in Organic Coatings, 64(4), 383-386.

Ramanan, G. and S. Shanavas, Multi-Objective Optimization of Machining Parameters for AA7075 Metal Matrix Composite Using Grey-Fuzzy Technique. International Journal of Applied Engineering Research, 2017. 12(8): p. 1729-1735.

Saravanan, K., Sathiyanarayanan, S., Muralidharan, S., Azim, S. S., & Venkatachari, G. (2007). Performance evaluation of polyaniline pigmented epoxy coating for corrosion protection of steel in concrete environment. Progress in Organic Coatings, 59(2), 160-167.

Selvi, S. and Rajasekar, E., 2015. Theoretical and experimental investigation of wear characteristics of aluminum based metal matrix composites using RSM. *Journal of Mechanical Science and Technology*, *29*(2), pp.785-792.

Senthilkumar, N., J. Sudha, and V. Muthukumar, A grey-fuzzy approach for optimizing machining parameters and the approach angle in turning AISI 1045 steel. Advances in Production Engineering & Management, 2015. 10(4): p. 195-208.

Shuvho, M. B. A., Chowdhury, M. A., Hossain, N., Roy, B. K., Kowser, M. A., & Islam, A., 2020, Tribological study of Al-6063-based metal matrix embedded with SiC–Al 2 O 3–TiO 2 particles. SN Applied Sciences, 2(2), 287.

Shuvho, M. B. A., Chowdhury, M. A., KCHAOU M., Rahman A., Islam M. A., 2020, Surface Characterization and Mechanical Behavior of Aluminum Based Metal Matrix Composite Reinforced with Nano Al2O3, SiC, TiO2 Particles. Chemical Data Collections, Accepted.

Shuvho, B. A., Chowdhury, M. A., & Debnath, U. K. (2019). Analysis of Artificial Neural Network for Predicting Erosive Wear of Nylon-12 Polymer. Materials Performance and Characterization, 8(1), 288-300.

Soy, U., Demir, A. and Findik, F., 2011. Friction and wear behaviors of Al- SiC- B4C composites produced by pressure infiltration method. *Industrial Lubrication and Tribology*.

Thompson, J.K., Li, W., Park, S.J., Antonyraj, A., German, R.M. and Findik, F., 2009.

Utilisation of silicon rubber to characterise tool surface quality during die compaction. *Powder metallurgy*, *52*(3), pp.238-243.

Tzeng, C.-J., et al., 2009, Optimization of turning operations with multiple performance characteristics using the Taguchi method and Grey relational analysis. Journal of materials processing technology, 209(6): p. 2753-2759.